

Figure 1. Static and spinning oxygen-17 Fourier transform NMR spectra of some inorganic oxides and oxyanions at 11.7 T (corresponding to an ^{17}O Larmor frequency of 67.8 MHz) together with the spectral simulation of a covalent (ether) oxygen NMR spectrum. (A) Static MgO , 39 scans, recycle time = 10 s. (B) MASS MgO at 4.5 kHz, 12 scans, recycle time = 30 s. (C) Static Al_2O_3 , 1350 scans, recycle time = 30 s. (D) MASS Al_2O_3 at 3.4 kHz, 195 scans, recycle time = 30 s. (E) Static SiO_2 , 10 scans, recycle time = 120 s. (F) VASS SiO_2 ($\theta = 75^\circ$) at 4.1 kHz, 47 scans, recycle time = 60 s. (G) Spectral simulation of an ether oxygen having $e^2qQ/h = 9.9$ MHz, $\eta = 0.6$, static spectrum. Values of between 10 and 100 Hz exponential line broadening were used to improve spectral signal-to-noise ratios. The scale is referenced to an external sample of tap water. Adapted from ref 4. The ppm values shown are those observed experimentally.

1 static and spinning ^{17}O NMR spectra of Mg^{17}O (Figure 1A,B), $\alpha\text{-Al}_2^{17}\text{O}_3$ (Figure 1C,D), and Si^{17}O_2 (low cristobalite, a framework or three-dimensional silicate, Figure 1E,F),⁴ in addition to a simulated spectrum of a typical covalent oxygen, that in xanthene (Figure 1G, ref 15). The results indicate a wide range of electric quadrupole coupling constants, varying from ~ 0 MHz in MgO to ~ 2.2 MHz for the oxygens in $\alpha\text{-Al}_2\text{O}_3$,¹⁶ ~ 5.8 MHz for the oxygens in SiO_2 ,^{4,17} and ~ 10 MHz for the oxygen in xanthene.¹⁵ Because of the potentially very large magnitude of the quadrupole interaction, the size of the electric field gradient at the ^{17}O nucleus determines, to a first approximation, the type of NMR spectrum to be obtained in solid-state ^{17}O NMR studies. For example, the ^{17}O MASS NMR spectrum of MgO contains a single line of $\lesssim 0.3$ ppm width, in the crystalline solid state, an extraordinarily narrow breadth due to the highly symmetric nature of the O^{2-} anion in the cubic MgO lattice.¹⁸ By contrast, the spectrum of SiO_2 ($e^2qQ/h \sim 5.8$ MHz) contains a well-resolved second-order powder pattern⁴ that is effectively narrowed under VASS conditions (Figure 1E,F, ref 4), while spectra of the purely covalent oxides (ethers) are essentially inaccessible with current operating field strengths, since e^2qQ/h values are ~ 10 MHz.¹⁵

The results of Figure 1 indicate that "high-resolution" ^{17}O NMR spectra of some oxides may be obtained but do not demonstrate the actual resolution of any nonequivalent oxygen sites. We therefore show in Figure 2 11.7-T ^{17}O MASS NMR spectra of

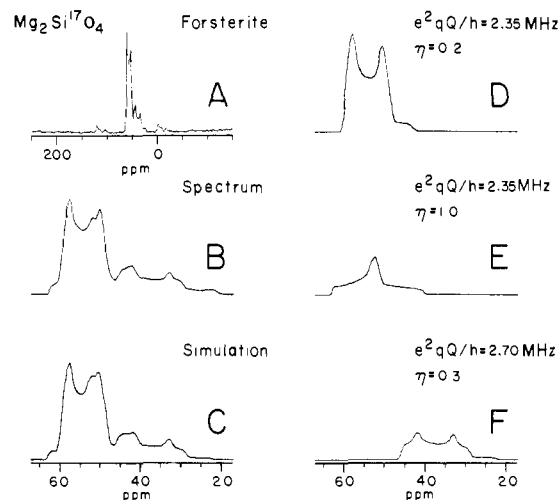


Figure 2. ^{17}O MASS NMR spectra (11.7 T), and spectra simulations, of $\text{Mg}_2\text{Si}^{17}\text{O}_4$ (forsterite). (A) MASS NMR spectrum, 370 scans at a 120-s recycle time using a $10\text{-}\mu\text{s}$ pulse excitation. (B) Expansion of A. (C) Spectral simulation of B using parameters of D-F. (D) Component 1, $\sigma_1 = 61$ ppm, $e^2qQ/h = 2.35$ MHz, $\eta = 0.20$, 50% intensity. (E) Component 2, $\sigma_1 = 62$ ppm, $e^2qQ/h = 2.35$ MHz, $\eta = 1.0$, 18% intensity in the center band. (F) Component 3, $\sigma_1 = 47$ ppm, $e^2qQ/h = 2.70$ MHz, $\eta = 0.3$ 18% intensity in the center band. Residual spectral intensities are located in the sidebands of components 2 and 3. The scales are referenced to an external sample of tap water; the errors in σ_1 are about ± 1 ppm.

the olivine type monosilicate, forsterite (Mg_2SiO_4), in which considerable structure is apparent, Figure 2A. The results of Figure 2A strongly suggest that at least three types of non-equivalent oxygen are present per SiO_4^{4-} unit, and in Figure 2B,C, we show an expansion of the center-band resonances of forsterite (Figure 2B), together with a spectral simulation of the line shape observed (Figure 2C). The results of the simulation indicate that there are three types of oxygen present, characterized by isotropic chemical shifts, quadrupole coupling constant, and electric field gradient tensor asymmetry parameters of 61 ppm, 2.35 MHz, and 0.2 (2 oxygens, Figure 2D), 62 ppm, 2.35 MHz, and 1.0 (1 oxygen, Figure 2E), and 47 ppm, 2.70 MHz, and 0.3 (1 oxygen, Figure 2F). Thus, the results of Figure 2 indicate that well-resolved oxygen-17 NMR spectra of simple oxyanions, containing non-equivalent oxygen atoms, may be readily observed by means of high-field MASS NMR techniques.

In principle, ab initio calculations should readily provide the desired quadrupole coupling constant (or electric field gradient tensor) information required for at least a preliminary prediction of the nature of the solid-state ^{17}O NMR spectra of any given oxide or oxyanion. In the absence of such results, however, we have found that an empirical relation based on the ionic character of the cation-oxygen bonds, obtained by means of the Pauling electronegativities, gives a useful estimate of the magnitude of e^2qQ/h to be expected in a given bonding situation. Results are shown in Figure 3 for MgO , K_2WO_4 , ZnO , Mg_2SiO_4 , $\text{CaMgSi}_2\text{O}_6$, $\alpha\text{-Al}_2\text{O}_3$, B_2O_3 , low cristobalite, H_2O , 2,5-dichlorohydroquinone, *p*-chlorophenol, tetrachlorohydroquinone, xanthene, tetrahydropyran, and *N*-methyl syndone.¹⁹ Percent ionic characters for the nonsymmetric interactions are average values based on the two strongest interactions, e.g., W-O and O-K in K_2WO_4 , C-O and O-H in tetrachlorohydroquinone, and so on.

Although very approximate, we believe the results of Figure 2, which may be represented as

$$e^2qQ/h \text{ (MHz)} = -0.203I(\%) + 14.78 \quad (1)$$

where I is the ionic character in percent and the correlation coefficient is ~ 0.96 , are a useful initial guide as to what oxides

(15) Hsieh, Y.; Koo, J. C.; Hahn, E. L. *Chem. Phys. Lett.* **1972**, *13*, 563.

(16) Brun, E.; Derighetti, B.; Hundt, E. E.; Niebuhr, H. H. *Phys. Lett.* **1970**, *31A*, 416.

(17) Bray, P. J.; Bucholtz, F.; Geissberger, A. E.; Harris, I. A. *Nucl. Instrum. Methods* **1982**, *199*, 1.

(18) Skinner, B. J. *Am. Mineral.* **1957**, *42*, 39.

(19) Kinzinger, J.-P. In "NMR Basic Principles and Progress"; Diehl, P., Fluck, E., Kosfeld, R., Eds.; Springer-Verlag: New York, 1982; Vol. 17, p 1.

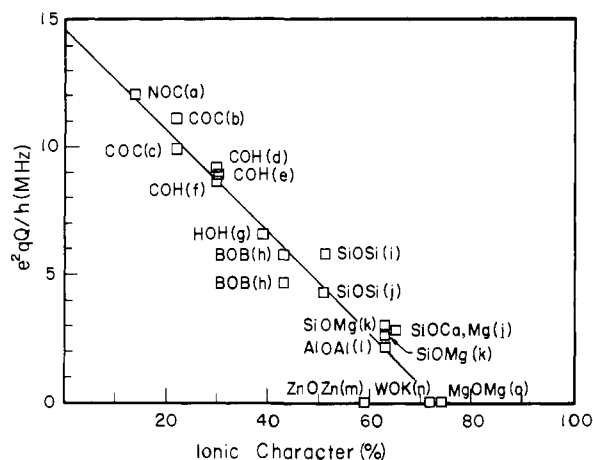


Figure 3. Plot of ^{17}O electric quadrupole coupling constant (e^2qQ/h , MHz) vs. average percent ionic character for a series of A-O-B fragments, where A and B are cations. The experimental e^2qQ/h values are for a series of oxides or simple oxyanions. The percent ionic character is the arithmetic mean of the single-bond values obtained from the Pauling electronegativities of elements A, B, and O. Species more covalent than SiO_2 are best studied by NQR or wide-line NMR methods, while more ionic systems are amenable to "high-resolution" solid-state MASS and VASS NMR techniques. The straight line is the least-squares fit of the data to eq 1. Compounds used were as follows: (a) *N*-methylsyndone, (b) tetrahydropyran, (c) xanthene, (d) tetrachlorohydroquinone, (e) 2,5-dichlorohydroquinone, *N*-methylsyndone, *p*-chlorophenol, (g) normal hexagonal ice, (h) B_2O_3 , (i) low cristobalite, (j) diopside, (k) forsterite, (l) Al_2O_3 , (m) zinc oxide, (n) potassium tungstate, (o) magnesium oxide.

or oxyanions are likely candidates for high-resolution solid-state NMR studies.

For example, at 11.7 T (corresponding to an ^{17}O resonance frequency of 67.8 MHz), the results of Figures 1-3 indicate that elements with electronegativities in excess of ~ 1.8 , bound to oxygen, may preclude the ready determination of high-resolution ^{17}O NMR spectra at currently available magnetic field strengths. Thus SiO_2 (Si EN = 1.8) has an e^2qQ/h value of ~ 5.8 MHz.^{4,17} At 67.8 MHz, this corresponds to a second-order powder pattern line breadth of the ($1/2, -1/2$) transition of ~ 20 kHz.^{3,11} By use of MASS, a complex line shape is obtained, however, by VASS, the first-order sideband is absent^{4,10,11} and a well-resolved center band is obtained (Figure 1). Clearly then, we would not expect it to be a straightforward matter to obtain high-resolution solid-state ^{17}O NMR spectra of more covalent species, e.g., B_2O_3 (B EN = 2.0), SO_3 phases (S EN = 2.5), or I_2O_5 (I EN = 2.5), while, as shown in Figures 1-3, spectra of more electropositive-element-containing species such as MgO and Al_2O_3 are readily obtained (Mg EN = 1.2, Al EN = 1.5).

While such predictions are clearly very crude, we believe they have some utility since they are simple to make and so far seem to be correct in indicating which oxides and oxyanions are suitable candidates for high-resolution MASS and VASS NMR in the solid state. Naturally, the presence of multiple (π) bonding will have additional complicating effects on the appearance of such ^{17}O NMR spectra, as shown below, and of course the simple relation can be forced to break down by invoking any array of ligands that gives perfect cubic symmetry.

Chemical Shift Effects in Solid-State ^{17}O NMR. The results of Figure 3 indicate that a wide variety of transition-metal oxides and oxyanions should be accessible to study by means of solid-state ^{17}O MASS and VASS NMR spectroscopy, since the electronegativities of these metals are all moderate, and at least in the oxyanions there will often be highly electropositive counterions present. In the absence of large quadrupole interactions, we may thus expect to see chemical shift resolved resonances, in addition to perhaps being able to obtain information on chemical shielding tensor interactions.

We show therefore in Figure 4 results on two typical transition-metal oxyanions, KMnO_4 and K_2WO_4 . In Figure 4A we

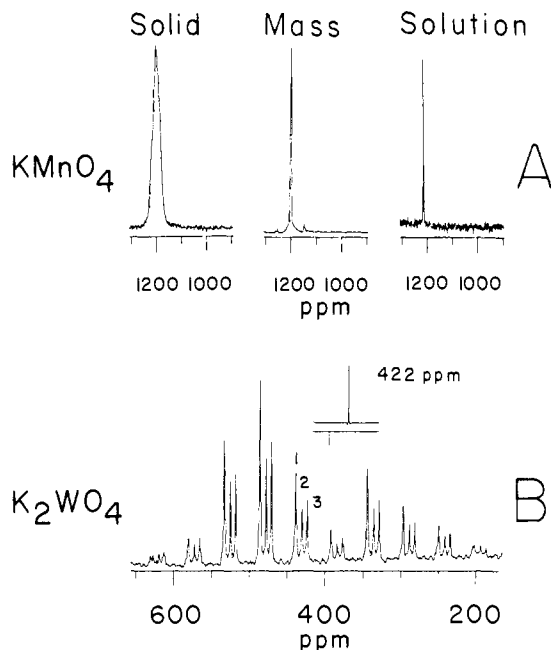


Figure 4. 67.8-MHz oxygen-17 Fourier transform NMR spectra (obtained at a magnetic field strength of 11.7 T) at 23 °C of (A) KMnO_4 as a static solid, while spinning at the "magic-angle", and as an aqueous solution, (B) K_2WO_4 , while spinning at the "magic-angle" and (inset) as an aqueous solution. All samples were ^{17}O enriched as discussed in the text. Typically, from 50 to 200 scans, at a 5-30-s recycle time, were acquired with $\sim 90^\circ$ pulse excitation. The MASS spinning rates were 3.6 (KMnO_4) and 3.2 kHz (K_2WO_4). In K_2WO_4 , all three crystallographically nonequivalent oxygen atoms are resolved. The numerous sets of resonances in B are due to a large ^{17}O chemical shift anisotropy and are generated via the sample-spinning process.

present the 67.8-MHz ^{17}O NMR spectrum of $\text{KMn}^{17}\text{O}_4$, both as a static crystalline solid, under 3.6-kHz "magic-angle" rotation, and as an aqueous solution. The line width of the static solid (~ 2.4 kHz, ~ 35 ppm) is due to a combination of K, Mn, and O dipole-dipole, second-order quadrupole, chemical shift anisotropy, chemical shift nonequivalence, and Mn-O indirect spin-coupling interactions. A rather featureless line is obtained (as with the ^{55}Mn resonance in KMnO_4 , ref 6, 11). Upon MASS, a narrow (~ 400 Hz, ~ 6 ppm) symmetric resonance at 1197 ppm downfield from external H_2^{17}O is obtained (in contrast to the characteristic line shape observed for ^{55}Mn in KMnO_4 , due to a second-order quadrupole interaction), indicating that e^2qQ/h is ≤ 0.4 MHz. The residual line breadth is considerably greater than that for $\text{KMn}^{17}\text{O}_4$ in aqueous solution (Figure 4A), but we cannot accurately deduce the relative contributions of the residual interactions. Note that each ^{17}O nucleus appears essentially magnetically equivalent in the rotating solid, consistent with the X-ray structural determination.²⁰

In sharp contrast to the results of Figure 4A we show in Figure 4B solution and crystal MASS NMR spectra of $\text{K}_2\text{W}^{17}\text{O}_4$. Clearly, the MASS NMR spectra of Figure 4A,B contain a number of remarkable differences. First, the spectrum of Figure 4B contains 10 groups of three lines. The frequency separations between the 10 groups correspond to the spinning frequency (3.2 ± 0.1 kHz) and change with spinning rate, while the separations between the three peaks remain constant. Thus, peaks 1, 2, and 3 represent the isotropic chemical shifts of the three nonequivalent oxygens in the WO_4^{2-} ion.²¹ The sum of the intensity of peak 1 and its sidebands is twice that of either peak 2 or 3 and their respective sidebands, thus peak 1 almost certainly corresponds to the two crystallographically equivalent oxygens in the WO_4^{2-} ion.²¹

(20) Palenik, G. J. *Inorg. Chem.* **1967**, *6*, 503.

(21) Koster, A. S.; Kools, F. X. N. M.; Rieck, G. D. *Acta Crystallogr., Sect B* **1969**, *B25*, 1704.

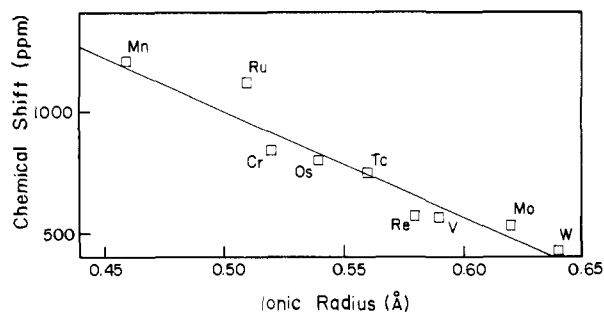


Figure 5. Plot of ^{17}O (solution) chemical shift (ppm from H_2^{17}O) vs. (crystal) cation ionic radius (\AA) for a series of oxides and oxyanions isoelectronic with MnO_4^- . The straight line is the least-squares fit of the data to eq 2 in the text. Ionic radii from: Kordes, E. *Z. Phys. Chem., Abt. B* **1939**, *43*, 213. Ahrens, L. H. *Geochim. Cosmochim. Acta* **1952**, *2*, 155.

From Figure 4B we find that the isotropic chemical shifts of the ^{17}O nuclei in K_2WO_4 are 437, 429, and 422 ± 1 ppm from external H_2^{17}O . In addition, analysis of the sideband intensity ratios of peaks 1, 2, and 3 as a function of spinning speed according to the method of Herzfeld and Berger²² yields the following *chemical shift tensors* for peaks 1, 2, and 3: $\sigma_{11}^1 = 564$, $\sigma_{22}^1 = 530$, and $\sigma_{33}^1 = 217$ ppm; $\sigma_{11}^2 = 567$, $\sigma_{22}^2 = 518$, and $\sigma_{33}^2 = 202$ ppm; $\sigma_{11}^3 = 561$, $\sigma_{22}^3 = 497$, and $\sigma_{33}^3 = 208$ ppm, where the values for σ^1 represent the shift tensor for the two equivalent oxygens in the WO_4^{2-} ion. This is the first observation of solid-state ^{17}O chemical shielding tensors we are aware of. The mean ^{17}O solid-state chemical shift of peaks 1 (2 oxygens), 2, and 3 is 431 ± 1 ppm, in good agreement with the solution value (422 ppm, Figure 4B; 420 ppm, ref 23).

The widths of the individual peaks in Figure 4B are somewhat narrower than with KMnO_4 , due in part we believe to the absence of an abundant spin species (^{55}Mn is 100% abundant, $I = 5/2$; ^{183}W is 14% abundant, $I = 1/2$).

The results of Figure 4A,B indicate that very narrow line widths may be obtained for some oxyanions, because of small (a few hundred kilohertz) e^2qQ/h values, due presumably to relatively weak M-O bonds.

In order to once again make a perhaps more chemically useful interpretation of at least some of the large differences in the NMR parameters (chemical shifts) observed for the two isoelectronic species (MnO_4^- , 1197 ppm; WO_4^{2-} , 431 ppm), we now discuss briefly the topic of ^{17}O NMR chemical shifts.

As is well-known, for most of the heavier elements the paramagnetic term, σ_p , dominates the shielding of a given nucleus. As originally pointed out by Freeman et al.,²⁴ a linear relation between NMR frequency and the wavelength of the lowest frequency optical absorption (at least for octahedral Co(III) complexes) exists, as it does for a series of oxyanions.²³ Carrington et al.^{25,26} observed a similar linear relationship between the first absorption maxima of a series of isoelectronic transition-metal oxides and oxyanions (MnO_4^- , RuO_4 , CrO_4^{2-} , OsO_4 , TcO_4^- , VO_4^{3-} , ReO_4^- , MoO_4^{2-} , WO_4^{2-}) and cation ionic radius. In addition, we and others^{13,27} have recently observed a linear relationship between Si-29 chemical shift and Si-O bond length (or cation-oxygen bond energy) in a variety of silicates, and there naturally exists a relationship between ionic radius and bond length for a series of

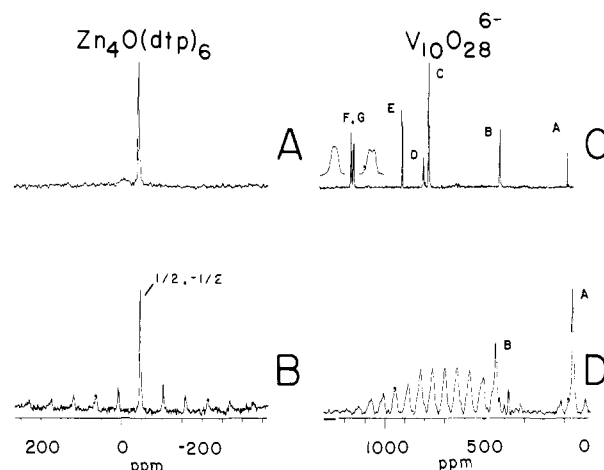
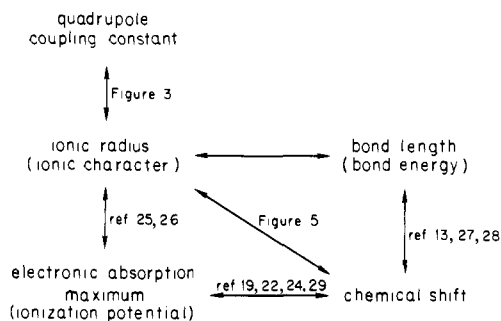


Figure 6. 67.8-MHz oxygen-17 Fourier transform NMR spectra of (μ_4 -oxo)hexakis(μ -*O,O*-diisopropylphosphorodithioato)tetrzinc (basic zinc dithiophosphate, $\text{Zn}_4\text{O}(\text{dtp})_6$) and ammonium and cesium decavanadates ($\text{V}_{10}\text{O}_{28}^{6-}$). (A) $\text{Zn}_4\text{O}(\text{dtp})_6$ in CHCl_3 solution, 697 scans at a 5-s recycle time. (B) Solid $\text{Zn}_4\text{O}(\text{dtp})_6$, MASS NMR at 3.7 kHz, 2260 scans at a 5-s recycle time. (C) $(\text{NH}_4)_6\text{V}_{10}\text{O}_{28}$ in H_2O solution, 258 scans at a 30-s recycle time. (D) $\text{Cs}_6\text{V}_{10}\text{O}_{28}$ MASS NMR at 4.2 kHz, 526 scans at a 120-s recycle time.

structurally similar compounds. These various empirically established relationships are illustrated below:



It thus seems plausible to expect a correlation between cation ionic radius and oxygen-17 chemical shift in a series of isoelectronic structures, and the results of Figure 5 for a series of group 5B, 6B, 7B, and 8 oxides and oxyanions show that this is indeed the case. The results are fitted by

$$\delta \text{ (ppm)} = -4394r \text{ (\AA)} + 3205 \quad (2)$$

with a correlation coefficient of 0.92. We believe this and other similar curves may be of use in predicting ^{17}O chemical shifts, both in solution and in the crystalline solid state. Indeed, the correlation shown above indicates a possible error in the reported chemical shift of MoO_4^{2-} reported in ref 19 and that the correct value is 530 ppm (ref 23 and our unpublished results), both in solution and in the crystalline solid state.

Results on More Complex Species. The results of Figures 1-5 were obtained on rather simple oxides and oxyanions. We show therefore in Figure 6 ^{17}O solid-state MASS NMR spectra of two more complex species: a basic zinc dithiophosphate ($(\mu_4\text{-}^{17}\text{O})$ -oxo)hexakis(μ -*O,O*-diisopropylphosphorodithioato)tetrzinc and cesium decavanadate ($\text{Cs}_6\text{V}_{10}^{17}\text{O}_{28}$), a polyoxy anion related to the naturally occurring mineral, pascoite ($\text{Ca}_3\text{V}_{10}\text{O}_{28} \cdot 17\text{H}_2\text{O}$).

The basic zinc dithiophosphate, $\text{Zn}_4\text{O}(\text{dtp})_6$, is thought to have a structure similar to that of the basic beryllium and zinc acetates,³⁰ containing a tetrahedral μ_4 -oxo group. On the basis of symmetry grounds alone, we might thus expect $e^2qQ/h \sim 0$, and the results of Figure 6 are consistent with this expectation. The ^{17}O MASS NMR spectrum (Figure 6B) contains a narrow center band (width ≤ 200 Hz) at -48.8 ppm, while the solution spectrum

(22) Herzfeld, J.; Berger, A. E. *J. Chem. Phys.* **1980**, *73*, 6021.
 (23) Figgis, B. N.; Kidd, R. G.; Nyholm, R. S. *Proc. R. Soc. London, Ser. A* **1962**, *269*, 469.
 (24) Freeman, R.; Murray, G. R.; Richards, R. E. *Proc. R. Soc. London, Ser. A* **1957**, *242*, 455.
 (25) Carrington, A.; Schonland, D.; Symons, M. C. R. *J. Chem. Soc.* **1957**, 659.
 (26) Carrington, A.; Symons, M. C. R. *J. Chem. Soc.* **1960**, 889.
 (27) Higgins, J. B.; Woessner, D. E. *EOS, Trans. Am. Geophys. Union Abstr.* **1982**, *63*, 1139.
 (28) Grimmer, A.-R.; Peter, R.; Fechner, E.; Molgedey, G. *Chem. Phys. Lett.* **1981**, *77*, 331.
 (29) Tosselli, J. A., private communication.

(30) Bridger, R. F., 24th Experimental NMR Conference, Asilomar, CA, April 10-14, 1982, Abstract B-3.

(Figure 6A and ref 30) contains a very narrow resonance at -48 ppm.³⁰ The additional sideband features present in Figure 6B arise, we believe, from the satellite ($\pm 1/2 \leftrightarrow \pm 3/2$; $\pm 3/2 \leftrightarrow \pm 5/2$) transitions. Similar results are predicted for the basic beryllium and zinc acetates and for the μ_6 -oxo atoms in the $V_{10}O_{28}^{6-}$ ion. Such predictions are borne out for O_A (see, e.g., ref 31 for nomenclature) in the $V_{10}O_{28}^{6-}$ ion, as shown in Figure 6.

In Figure 6C we show the spectrum of the $V_{10}O_{28}^{6-}$ ion in H_2O solution, and the integrated peak intensities are as expected:³¹ O_A (2), O_B (4), O_C (8), O_D (2), O_E (4), O_F (4), and O_G (4). All lines are quite narrow, except for $O_{F,G}$ which show partially resolved splittings, presumably due to $^1J_{SiV-17O}$ interactions. In the crystalline solid state (as the Cs salt rather than the NH_4^+ salt to reduce dipolar interactions) the overall spectrum is, however, quite different, Figure 6D. The μ_6 -oxo atom (O_A) has a very similar chemical shift (52.0 ppm) to that observed in solution (63.3 ppm). This result is consistent with the observation of a very sharp solution line width for O_A ³¹ (Figure 6C) and simply indicates a very high symmetry O^{2-} environment, as in the case of the $Zn_4O(dtp)$ species (Figure 6B). However, the only other resonance in the solid-state ^{17}O NMR spectrum of $Cs_6V_{10}O_{28}$ to clearly correspond to the solution-state chemical shift and line width is that of O_B , the μ_3 -O site. The more complex features of the $Cs_6V_{10}O_{28}$ spectrum will be discussed in more detail elsewhere.³²

Concluding Remarks. The results presented in this paper represent our first attempts at obtaining and interpreting the ^{17}O solid-state NMR spectra of a variety of oxides and oxyanions, which we have carried out in order to provide a basis for further studies of related systems of catalytic and geochemical interest. Our results indicate that a very wide range of quadrupole coupling, chemical shift, and chemical shift anisotropy values are to be expected for ^{17}O nuclei in solids. We have presented results which indicate that species more covalent than silica (Si-O-Si) are unlikely to be amenable to investigation with either ^{17}O MASS or VASS NMR techniques with currently available magnetic field strengths. For the silicates themselves, however, even modest increases in magnetic field strengths (e.g., 500 \rightarrow 600 MHz 1H

resonance frequency) will provide very significant ($\sim 50\%$) increases in spectral resolution, since for such systems resolution improves *quadratically* with increasing magnetic field strength.^{34,11}

Our results with the simple SiO_4^{4-} and WO_4^{2-} species illustrate the potential power of solid-state ^{17}O NMR spectroscopy. Even in very simple oxyanions we have shown that nonequivalent oxygen atoms may be resolved, and that quadrupole coupling constants, chemical shift tensors, and their asymmetry parameters may be determined. Our results indicate that very large chemical shift anisotropies (some 300 ppm) are observed with some oxyanions (which also have vanishingly small e^2qQ/h values), and our unpublished results on metal carbonyls³³ indicate that $\Delta\sigma$ values as large as 600 ppm are to be expected for some species. We thus believe that the results presented in this publication indicate a very promising future for ^{17}O solid-state NMR studies in chemistry and geochemistry, especially for the structural analysis of systems not readily investigated by single-crystal X-ray diffraction techniques, by means of future detailed analyses of solid-state chemical shift and quadrupole coupling constant information.

Acknowledgment. We thank R. F. Bridger of the Mobil Research and Development Corporation, Princeton, NJ, for the sample of ^{17}O -labeled $Zn_4O(dtp)_6$, R. J. Kirkpatrick, for the sample of ^{17}O -labeled forsterite, and D. M. Henderson and R. J. Kirkpatrick for useful discussions. This work was supported in part by NIH, NSF, the American and Illinois Heart Associations, and the Mobil Foundation, by an Arnold O. Beckman Research Award from the University of Illinois, and has also benefitted from facilities made available through the University of Illinois-National Science Foundation Regional NMR Instrumentation Facility.

Registry No. ^{17}O , 13968-48-4; B_2O_3 , 1303-86-2; $CaMgSi_2O_6$, 14483-19-3; Mg_2SiO_4 , 15118-03-3; Al_2O_3 , 1344-28-1; ZnO , 1314-13-2; K_2WO_4 , 7790-60-5; MgO , 1309-48-4; *N*-methylsyndone, 6939-12-4; tetrahydropyran, 142-68-7; xanthene, 92-83-1; tetrachlorohydroquinone, 87-87-6; 2,5-dichlorohydroquinone, 824-69-1; *p*-chlorophenol, 106-48-9; cristobalite, 14464-46-1; ice, 7732-18-5.

(31) Klemperer, W. G.; Shum, W. *J. Am. Chem. Soc.* 1977, 99, 3544.
(32) Schramm, S.; Oldfield, E., unpublished results.

(33) Keniry, M. A.; Shinoda, S.; Brown, T. L.; Oldfield, E., unpublished results.

Two-Dimensional Heteronuclear Chemical Shift Correlation Spectroscopy in Rotating Solids

James E. Roberts, Shimon Vega,[†] and Robert G. Griffin*

Contribution from the Francis Bitter National Magnet Laboratory, Massachusetts Institute of Technology, Cambridge, Massachusetts 02139. Received September 22, 1983

Abstract: Two-dimensional NMR methods for performing heteronuclear chemical shift correlation experiments in rotating solids are described. The general approach involves both homo- and heteronuclear decoupling during the evolution (t_1) period followed by a coherence transfer or mixing period (τ_{mix}) in which information is transferred between the spin reservoirs. During the detection (t_2) period heteronuclear decoupling is employed and the NMR signals are observed in the customary fashion. Several methods for coherence transfer are discussed, and it is concluded that the method of choice will likely be sample dependent. Three different classes of two-dimensional spectra will be observed in these experiments—containing sidebands in neither, one, or both spectral dimensions—and examples of each type are described. Finally, the occurrence of rotor frequency lines in multiple-pulse/magic-angle sample spinning 1H spectra is discussed.

Introduction

Despite the availability of sophisticated pulse sequences that attenuate the proton-proton dipolar interaction,¹ the task of obtaining high-resolution proton spectra of polycrystalline powders

remains difficult. The residual line widths obtained with multiple-pulse sequences during magic-angle sample spinning (MASS) are typically 2 ppm.²⁻⁴ When compared to the normal 10-15-ppm

[†] On leave from the Isotope Department, Weizmann Institute of Science, Rehovot, Israel.

(1) (a) Mehring, M. "High Resolution NMR in Solids", 2nd ed.; Springer-Verlag: Berlin, 1983. (b) Haebleren, U. "High Resolution NMR in Solids, Selective Averaging"; Academic Press: New York, 1976.